Revolutionary Aeropropulsion Concept for Sustainable Aviation: Turboelectric Distributed Propulsion

Hyun Dae Kim, James L. Felder, Michael T. Tong
NASA Glenn Research Center
Cleveland, Ohio, U.S.A.

and

Michael Armstrong
Rolls-Royce North America Technologies, Inc.,
Indianapolis, Indiana, U.S.A.

Abstract

In response to growing aviation demands and concerns about the environment and energy usage, a team at NASA proposed and examined a revolutionary aeropropulsion concept, a turboelectric distributed propulsion system, which employs multiple electric motor-driven propulsors that are distributed on a large transport vehicle. The power to drive these electric propulsors is generated by separately located gas-turbine-driven electric generators on the airframe. This arrangement enables the use of many small-distributed propulsors, allowing a very high effective bypass ratio, while retaining the superior efficiency of large core engines, which are physically separated but connected to the propulsors through electric power lines. Because of the physical separation of propulsors from power generating devices, a new class of vehicles with unprecedented performance employing such revolutionary propulsion system is possible in vehicle design. One such vehicle currently being investigated by NASA is called the "N3-X" that uses a hybrid-wing-body for an airframe and superconducting generators, motors, and transmission lines for its propulsion system. On the N3-X these new degrees of design freedom are used (1) to place two large turboshaft engines driving generators in freestream conditions to minimize total pressure losses and (2) to embed a broad continuous array of 14 motor-driven fans on the upper surface of the aircraft near the trailing edge of the hybrid-wing-body airframe to maximize propulsive efficiency by ingesting thick airframe boundary layer flow. Through a system analysis in engine cycle and weight estimation, it was determined that the N3-X would be able to achieve a reduction of 70% or 72% (depending on the cooling system) in energy usage relative to the reference aircraft, a Boeing 777-200LR. Since the high-power electric system is used in its propulsion system, a study of the electric power distribution system was performed to identify critical dynamic and safety issues. This paper presents some of the features and issues associated with the turboelectric distributed propulsion system and summarizes the recent study results, including the high electric power distribution, in the analysis of the N3-X vehicle.

Nomenclature

ADP	aerodynamic design point
BLI	boundary layer ingestion
BPR	bypass ratio
BSCCO	barium strontium calcium copper oxide
CFF	crossflow-fan
CMC	ceramic matric composites
eBPR	effective bypass ratio
GTOW	gross takeoff weight
HWB	hybrid-wing-body
LH_2	liquid hydrogen
MgB_2	magnesium di-boride
NOx	nitrogen oxides
NPSS	Numerical Propulsion System Simulation computer code
OEI	one-engine-inoperative
OPR	overall pressure ratio
PAI	propulsion airframe integration
RTO	rolling takeoff
TeDP	turboelectric distributed propulsion
TME	total mission energy
TOC	top-of-climb
TRL	technology readiness level
TSEC	thrust specific energy consumption
TSFC	thrust specific fuel consumption
WATE	Weight Analysis of Turbine Engines computer code

Introduction

The NASA Fundamental Aeronautics Program (FAP) has defined goals for the next three generations of aircraft identified as N+1, N+2, and N+3,[1] where each generation represents achieving a technology readiness level (TRL)[2] of 4 to 6 by the years 2015, 2020, and 2025 respectively. The current N+3 generation aircraft goals are a 52-dB cumulative noise reduction relative to FAA Stage 4 noise limits, an 80% reduction in NOx emissions below the ICAO Committee on Aviation Environmental Protection (CAEP)/6 levels during landing and takeoff (LTO) phases, and a 60% reduction in total mission fuel/energy consumption relative to the base in class current aircraft. Although it may not be feasible to meet all the goals simultaneously, multi-objective studies are being attempted to identify possible vehicle concepts that have the best potential to meet the combined goals. To meet these aggressive goals, drastic changes in vehicle and propulsion system designs are required.

One approach proposed by NASA and being examined by various groups is called "Turboelectric Distributed Propulsion (TeDP)."[3] Fig.1 shows a schematic of such system.
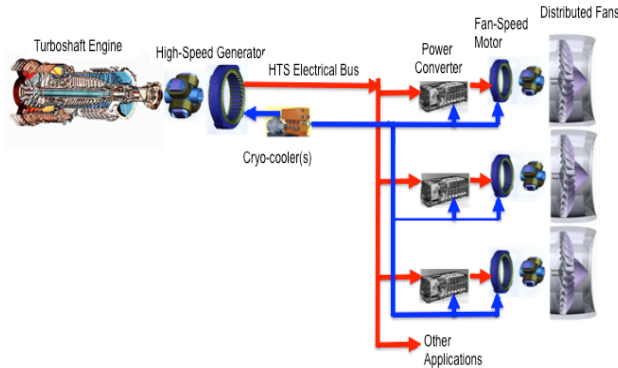

Figure 1: A schematic of turboelectric distributed propulsion (TeDP) system

The concept employs a number of high-power electric motors to drive the distributed propulsors. The power to drive these electric propulsors is generated by separately located gas-turbine-driven electric generators on the airframe. This arrangement enables the use of many small distributed propulsors, allowing a very high effective bypass ratio (eBPR), while retaining the superior efficiency of large core engines, which are physically separated but connected to the propulsors through high power electric transmission lines. The following are some of the features and issues associated with TeDP system.

- The use of electrical power transmission allows a high degree of flexibility in positioning the turboelectric generators and propulsor modules to the best advantage.
- Large combined fan areas from multiple small fans provide very high eBPR and low fan noise.
- Because the majority of the power is extracted from the engine core to power the electric fans, the core jet noise is substantially reduced because of low core jet exhaust velocity.
- In case of one-engine-inoperative (OEI) situation, the remaining operative turbogenerator still provides power to all operating electric fans for symmetric thrust. This feature greatly reduces or possibly eliminates the vertical tail, which is usually sized for an OEI situation on conventional aircraft sizing.
- Vehicle control could be achieved with a fast-response electric fan module. Since the exhaust air from the fan is "cold," and not "hot" combustion air from the core engine, thrust vectoring devices may employ conventional lightweight airframe materials.
- Electric components such as generators, motors, and transmission lines must be highly efficient and lightweight. Furthermore, the power distribution of multi-megawatts of electric power from the generators to the fan motors must be carefully considered and designed.
- Propulsion airframe integration (PAI) will play a greater role in achieving the N+3 goals because of the distributed thrust stream interacting with airframe.

One vehicle configuration currently being examined by a team at NASA is a hybrid-wing-body (HWB) aircraft integrated with the proposed TeDP system. Based on the recent development in lightweight, highly efficient superconducting technologies, NASA is continuing to perform a conceptual analysis of the proposed superconducting TeDP system on the vehicle named the "N3-X," and its results are summarized in the following sections.

N3-X Vehicle Description

The N3-X vehicle shown in Fig. 2 is conceptually similar to a previous study of a cruise-efficient short takeoff and landing (CESTOL)[3] airframe configuration with an integrated TeDP system. The vehicle uses the HWB airframe because of its high lift-to-drag ratio[4] and allows the distributed electric fans to ingest large amounts of thick upper fuselage boundary layer flow, resulting in significant

Turboshaft engine with superconducting generator

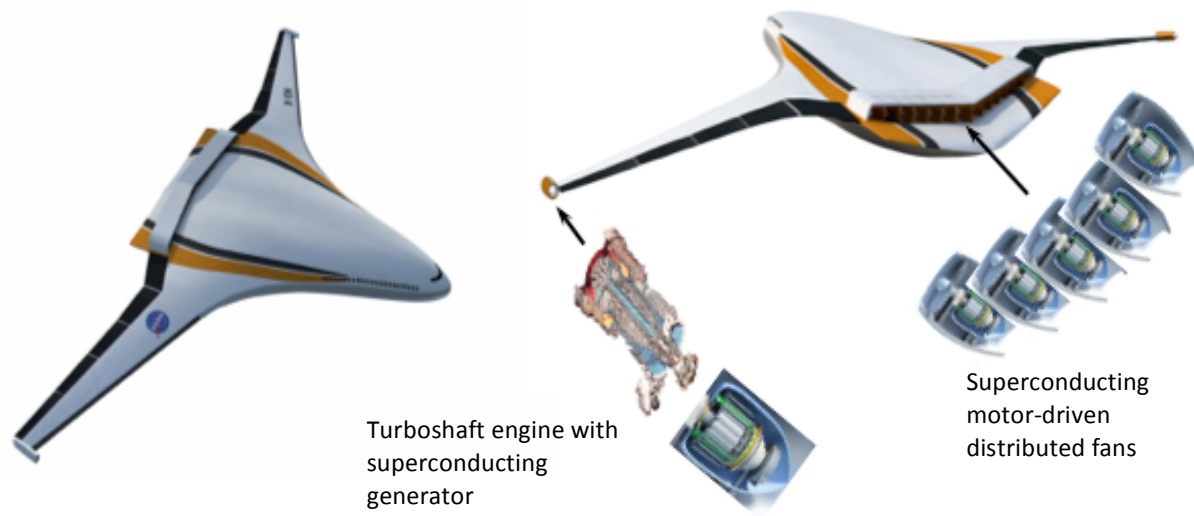Superconducting motor-driven distributed fans

Figure 2: N3-X vehicle using superconducting turboelectric distributed propulsion (TeDP) system

reduction in fuel burn and shielding of noise from the community below.[5] The airframe is derived from Boeing's N2A HWB configuration[6] with mission characteristics of a 7500-nmi range, a 118,000-lb payload capacity, and the ability to fly at an aerodynamic design point (ADP) of Mach 0.84 at 35,000 ft altitude. The propulsion system uses a lightweight, highly efficient superconducting electric system for motors, generators, and transmission lines.

In the aircraft configuration examined, the turbogenerators were located at the wing tips where the turbogenerators would experience undisturbed free-stream conditions and thus maximize the power of the turboshaft engine. In addition, the engine exhaust air disrupts the strong wing-tip vortex to effectively lower the induced drag of the vehicle. The fan modules were positioned in a continuous fan nacelle across the rear fuselage where they ingest the thick boundary-layer flow. This reduced the inlet drag of the propulsion system and filled the wake of the aircraft with fan discharge air, thereby reducing the drag of the vehicle. Because conventional pylons are not used in this configuration and the fact that the upper nacelle surface basically replaces the airframe surface that was originally there under the nacelle, it is expected that no significant external drag associated with the nacelle would be present.

The propulsion system shown in Fig. 2 employs 14 fans driven by superconducting electric motors with power provided by two separately located, superconducting electric generators based on a conventional turboshaft core engine design. The semi-embedded distributed fans are installed on the upper surface of the HWB airframe to ingest

significant amount of fuselage boundary layer flow to increase propulsive efficiency of the propulsion system. Ingesting the boundary layer reduces the average inlet velocity to less than the free-stream value and thus reduces the ram drag of the inlet. If the inlets can also be located far aft on the HWB center body airfoil section, the natural diffusion of the airframe will also reduce the velocity of air above the boundary layer. This further reduces inlet drag for inlets that project above the boundary layer height. To achieve the maximum boundary layer ingestion (BLI) benefits on the N3-X, the nacelle width is expanded as much as necessary on the top of the airframe. The current width is 65 feet across the area near the trailing edge of the upper fuselage.

Electric Power Distribution System

The N3-X employs a superconducting TeDP system and requires a careful consideration in the stability, transient response, control, and safety of its high-power electric grid. The TeDP's wholly superconducting electrical system must meet all steady-state and transient thrust requirements under the same reliability requirements as conventional propulsion systems. However, with distributed propulsion the overall propulsion system reliability is subject to additional electrical system failure scenarios, and these could introduce thrust losses. Additionally, this distributed propulsion system is tasked as an integral means for providing aircraft directional stability and control via differential thrust. Because of the flight-critical nature of this system, safety and reliability become the driving factors behind system design. Reliability and failsafe requirements must be met at minimal weight penalty

and acceptable levels of system complexity. Sufficient electrical system reliability is provided via the use of redundancy and system reconfiguration. Thrust requirements are reallocated and propulsive power is redirected during fault scenarios. Sufficient reliability can be achieved by radial or interconnected electrical distribution systems. A radial distribution system is illustrated in Figure 3. A radial system fulfills safety and reliability requirements with additional redundancy and weight, while an interconnected system can reduce redundancy and introduce additional complexity by requiring power to be rerouted.

The variable-frequency AC (alternating current) power signal generated by the superconducting generators driven by the turboshaft engines is converted to DC (direct current) via power converters. Fault isolation for the power generation equipment is provided via protection devices in conjunction with the power electronics of the converter. The protection systems include solid-state electrical contactors, superconducting fault current limiters, and the converter equipment itself. Superconducting fault current limiters may be advantageous between the generator and converter, depending on the fault-current carrying capability of both devices. Power is then transmitted from the wing-tip turbogenerators to the distribution system within the main body of the aircraft. Each central bus feeds multiple propulsors and is supported by an energy storage device to provide fill-in power and assist in voltage regulation.

Whereas in a conventional propulsion concept the engine provides thrust directly, the TeDP system requires several more layers of fail-safe devices to provide the same functionality. All power generation, conversion, distribution, and electrical support systems must be in operation to ensure nominal thrust availability. One fundamental advantage of this propulsion system is the inherent redundancy in propulsion devices. However, additional redundancy is required to provide power to these propulsors. Because of fail-safe operational requirements, the system will be over double the weight of an ideally operating TeDP system. Protection equipment alone accounts for 25% to 35% of the overall system weight.[7]

Voltage Level

Voltage levels on existing electrical systems for aircraft are relatively low compared to high-power terrestrial systems. Although ground-based power systems routinely operate at the kilovolt level, the highest accepted power distribution voltage for conventional transport aircraft is ±270 VDC. This conventional voltage limit was selected primarily because of voltage level limits derived from Paschen's Law.[8] At altitude, the low-pressure atmosphere decreases the voltage at which electrical arcing occurs. According to Paschen's Law, the minimum breakdown voltage for any pressure-distance product is approximately 327 V. Voltage levels below this value at high altitude will not breakdown in an air gap. Ground-based systems are not subject to the same breakdown voltage limits as systems at elevated altitude. Additionally, sophisticated insulation and shielding methods are applied to allow voltages higher than Paschen's limit. This 327-V limit was derived considering the
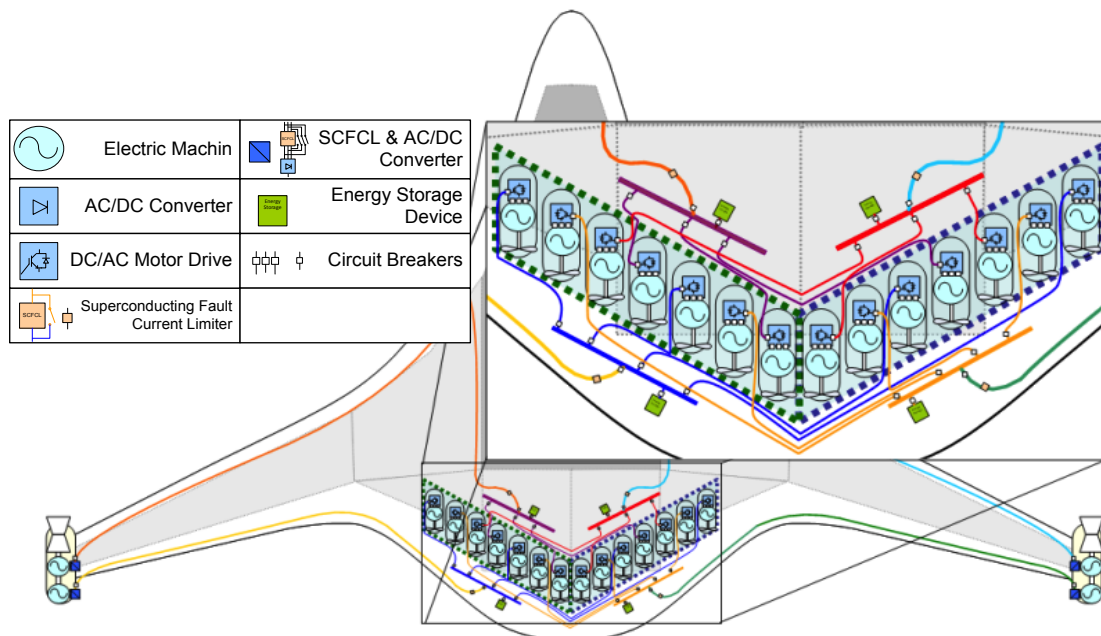

Figure 3: Baseline radial layout for TeDP electrical system

potential between two parallel, flat plats separated by air. As such, with advanced electrical system safety technologies, it is a highly conservative constraint placed on aircraft power systems. Cryogenically cooled high-voltage distribution systems are designed with high levels of protection against partial discharge. If properly designed for an aircraft-type environment, polymeric dielectrics' electrical properties tend to greatly benefit from the cryogenic temperatures.[9] Polymer dielectric strength can range from 10–15 kV per millimeter.[10] Epoxy-bound nanoparticles at cryogenic temperatures can range from 25-40 kV per millimeter.[11] The presence of a pressurized refrigerant itself provides some additional electrical insulation. Although both gaseous hydrogen and nitrogen have a lower minimum breakdown voltage than air[12], elevating the coolant pressures to 300 kPa increases the dielectric strength of the refrigerant to approximately 9 kV per millimeter for hydrogen-cooled machines,[13] and to 14 kV per millimeter for high-temperature superconducting machines cooled with liquid nitrogen[14]. In addition, liquid-nitrogen refrigerant has been shown to protect polymer electrical insulations against mechanical damage compared to gaseous nitrogen. Typical polymeric insulation materials increase in dielectric strength by 5–10× over room-temperature capabilities. To date, cables have been tested with pulsed potentials greater than 100 kV.[15] Although evolving, insulation design is progressing towards long-term stability and high-voltage capability.

To determine the optimal DC system voltage for minimum system weight or maximum power capability, a system-level study is necessary that considers the power densities, which are likely to be nonlinear, for each piece of equipment throughout the electrical system. Voltages are then selected for maximum power transfer capability or maximum power-to-weight ratio as illustrated in Ref. 16. However, such a study at the system level requires reasonable levels of knowledge regarding power densities for superconducting generators and motors, cable, fault-current limiters, circuit breakers, and

cryogenic converters. Other factors that should be considered when determining system voltage levels are contamination in the air gap, impact of vibration, abnormal system events, transient events,[17] and manufacturability of the equipment.

Yaw Control

The TeDP system offers unique opportunities for the flight control system. These opportunities include the elimination of the single engine out, asymmetric thrust, yaw moment requirements, and the reduction or removal of vertical surfaces intended to provide directional stability and control.

Traditionally, control surface sizing is driven in large part by the need to overcome the yaw moment generated during a worst-case, engine-out scenario.[18] A single-engine failure scenario remains one of the most sizing-critical failure scenarios for the TeDP system. However, delivering thrust in a distributed fashion allows for intelligent routing of power during a failure condition to alleviate the challenges associated with asymmetric thrust. Each generator provides power to multiple propulsors during failure conditions. Additionally, each propulsor utilizes alternative power sources for fill-in power. This is provided by temporary fill-in power from energy storage and interconnections with the other buses. As such, fail-safe power is provided from the other power turbogenerator or from energy storage devices on the central distribution buses.[19] If the propulsion system is able to maintain symmetric thrust, the control surface sizes for the aircraft may be reduced, since they are no longer configured to handle asymmetric thrust sizing cases.

Initial steps to providing consistent symmetric thrust involve the intelligent assignment of propulsors to distribution buses. Figure 4 illustrates the bus assignment of 14 propulsors on four power distribution buses. Configured in this fashion a bus, transmission line, generator, or engine failure will not produce adverse yawing conditions. The effect of a loss of power to a given bus may also be mitigated
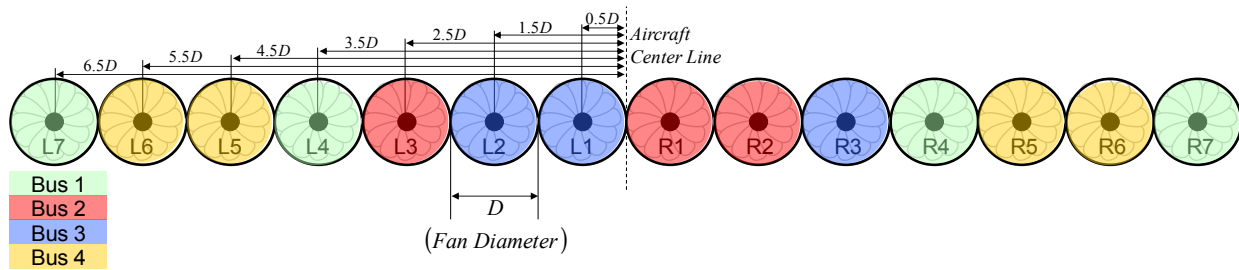

Figure 4: Propulsor bus assignment to mitigate asymmetric thrust during TeDP component failure scenarios

via secondary feeder lines to alternative buses during system failure scenarios.

Additional aerodynamic and flight control efficiency improvements may be realized by providing differential thrust for directional control. Depending on the response rate of the electric machines and integrated controls, the role of differential thrust may range from providing yaw trimming to active stability augmentation. For the propulsion system to handle various transient thrust and failure scenarios and still provide the necessary yawing moment to control the airplane, a significant level of complexity would have to be added to both vehicle and engine hardware and software.

Propulsion Cycle Analysis

The baseline propulsion system cycle was constructed using the Numerical Propulsion System Simulation (NPSS)[20-21] code with all the component performance parameters set at values reflecting the best values anticipated to be at TRL of 4-6 by the year 2025. Table 1 contains a list of the key parameters and the baseline values.

Table 1: Baseline values of key input parameter

Component	Parameter	Baseline Design Value
Propulsor Inlet	dP/P	0.50%
Fan	Fan pressure ratio (FPR)	1.3
Fan	Undistorted adiabatic efficiency	95.35%
Fan	Boundary layer ingestion distortion efficiency penalty	1%
CompL	Polytropic efficiency	93.25%
CompH	Polytropic efficiency	93.25%
CompH	Max exit total temperature (T3)	1,350 °F (1,810 °R)
TurbH	Max CMC material temperature	3,000 °F (3,460 °R)
TurbH	Polytropic efficiency	93.00%
TurbL	Polytropic efficiency	93.00%
TurbP	Polytropic efficiency	92.40%
Motor	Efficiency for 4064 hp and 4400 rpm	99.97%
Generator	Efficiency for 28505 hp and 8000 rpm	99.98%
Inverter	Efficiency for 4064 hp inverter	99.93%

The fan efficiency is stated as the undistorted efficiency, which is what the efficiency is anticipated to be if the fan were used in a standard pylon mounted turbofan with a circular pitot inlet ingesting undisturbed freestream air. The boundary layer distortion penalty is the estimated reduction of the undistorted adiabatic efficiency due to the distortion effects of the ingested boundary layer and the off-set

from 2-D to circular inlet. The baseline estimate for the fan efficiency penalty due to distortion, in keeping with the ground rule of selecting the most optimistic value anticipated by 2030, is set to 1%.[22]

The compressor and turbine polytropic efficiency values represent the best consensus values for N+3 timeframe turbomachinery devices. The hot section of the turboshaft engine is assumed to be composed entirely of uncooled ceramic matric composites (CMC) blades and stators. The turbine disks are assumed to be metallic and require about 7% of the main flow for cooling.

The electrical transmission system is assumed to be composed of superconducting motors and generators with superconducting transmission cables and cryogenic (but not superconducting) inverters and rectifiers. The losses in the electrical system are dominated by AC losses in the motor and generator stators and the DC-AC losses in the inverters. The inverter is not a superconducting device, however reducing the temperature to below 100 K is calculated to reduce the losses in this device to a very small percentage of the power passing through it. The entire electric transmission system is assumed to be contained within a single cryostat with ambient temperature penetration only at the motor and generator drive shafts and control leads. Modern vacuum insulation systems reduce ambient heat leak to a level where it is dominated by the losses in the motors, generators and inverters. Until the fidelity of the estimates of these larger losses is improved the ambient heat leak can be safely ignored.

Two superconducting materials were examined, barium strontium calcium copper oxide (BSCCO) and magnesium diboride (MgB_2). BSCCO has a critical temperature of 108 K with a working temperature in the TeDP system of 58 K. The MgB_2 has a critical temperature of 39 K with a working temperature of 28 K. Two different cryogenic cooling systems were also examined, an electric-motor-driven, reverse Brayton cycle refrigerator, referred to as a cryocooler, and direct cooling with liquid hydrogen (LH_2). Both cooling systems are capable of cooling either superconducting material. However, since the power and weight of a cryocooler for a given amount of energy removal rise very rapidly with reduction in cold-side temperature, the BSCCO system with the higher working temperature was cooled with the cryocooler. The boiling point of liquid hydrogen is 21 K at ambient pressure, which is compatible with the 28 K working temperature of MgB_2, and so the MgB_2 system was cooled with LH_2.

After LH$_2$ has been used to cool the superconducting components and the cryogenic inverters, the hydrogen is compressed and burned in the turboshaft engines to supply a portion of the fuel. The energy available from the hydrogen used for cooling is about 10% of that required driving the generators, so 90% of the total fuel energy comes from conventional jet fuel. The amount of hydrogen for each operating condition is determined by the amount of heat to be removed, and so the proportion of total energy coming from hydrogen is not fixed. Hydrogen has about 2.7 times lower heating value than jet fuel; thus, adding 1 pound of hydrogen reduces the amount of jet fuel by 2.7 pounds.

Tables 2 and 3 contain the performance of the TeDP system on the N3-X at the key operating points of a sea level, Mach 0.24, takeoff condition referred to as the rolling-takeoff (RTO) condition and a 34,000-ft, Mach-0.84, top-of-climb (TOC) condition that is the aerodynamic design point (ADP). The engine cycle was designed with a maximum turbine inlet temperature that is 100 °R less than the maximum

Table 2: 34,000 ft, M0.84, ISA day top-of-climb (TOC) performance summary

TOC	N3-X/BSCCO	N3-X/MgB$_2$
Fn - lbf	35,465	33,405
TSFC – lbm/hr/lbf	0.3412	0.3125
TSEC – BTU/s/lbf	1.761	1.727
BPR	29	30.1
OPR	83.5	84.3
T3 – °R	1,680	1,683
T4 –°R	3,260	3,260
Wair – lbm/s	3,881	3,696
Vbypass-Inlet-ft/s	736	735
Vbypass-Nozzle-ft/s	990	989
Vcore-Inlet-ft/s	821	821
Vcore-Nozzle-ft/s	1,371	1,359

Table 3: Sea level, M0.24, ISA+27 °R rolling-takeoff (RTO) performance summary

RTO	N3-X/BSCCO (installed)	N3-X/MgB$_2$ (installed)
Fn – lbf	94,161	85,846
TSFC – lbm/hr/lbf	0.2356	0.2174
TSEC – BTU/s/lbf	1.216	1.1937
BPR	35.3	36.1
OPR	57	57.3
T3 –°R	1,804	1,808
T4 - °R	3,360	3,360
Wair – lbm/s	8,361	7,823
Vbypass-Inlet – ft/s	253	253
Vbypass-Nozzle – ft/s	608	602
Vcore-Inlet – ft/s	274	274
Vcore-Nozzle – ft/s	758	745

CMC material temperature limit. The difference in thrust between the BSCCO and MgB$_2$ systems at both the TOC and the RTO is due to the lower thrust specific fuel consumption (TSFC) of the hydrogen cooled system that leads to a lower fuel load which in turn leads to a lighter aircraft, as seen in the section "N3-X Mission Performance". The lower TSFC is due to the higher lower heating value of hydrogen (51,591 BTU/lb), which is used as a portion of the total fuel after it is used as a coolant, compared to jet fuel (18,580 BTU/lb). It should be noted that the data in these tables represent the installed performance of the propulsion system. Because of the highly integrated nature of the propulsion system there is essentially no uninstalled performance that can be quoted.

Propulsion System Flow-Path Conceptual Design and Weight

The TeDP system weight calculation accounts for the weights of turboshaft engines, propulsors, and the associated electrical components such as superconducting generators, superconducting motors, superconducting transmission lines, cryocoolers, and cryogenic inverters. For the propulsion system weight estimation, the NASA software tool called Weight Analysis of Turbine Engines (WATE++)[23,24] was used to create engine architectures that could achieve the engine thermodynamic cycle detailed above. Since WATE's original release in 1979, substantial improvements have been made to enhance its capability and improve its accuracy. Many of the empirical relationships have been replaced with analytical weight and dimension calculations. An approach is used where the stress level, maximum temperature and pressure, material, geometry, stage loading, hub-tip ratio, blade/vane counts, and shaft speed are used to determine the component weight.

The cycle data required for WATE execution, such as airflow, temperatures and pressures, pressure ratios, etc., were derived from the NPSS cycle model output. Both the ADP and off-design cases were used to encompass the maximum performance level required for each engine component. CMCs were assumed for the turboshaft engine turbine vanes and blades to accommodate higher engine operating temperatures and to reduce the weight. Polymer composite was chosen for the propulsive fan blades and nacelles for both the turboshaft engines and the propulsors.

The length of each of the BLI inlets was set at about 1.5 fan diameters to provide the space for flow control that would be used to reduce flow distortion. About 25% of each fan diameter is embedded in the

airframe, to reduce the ram drag. The lengths of the propulsor nozzles were set at 1 fan diameter, and thrust vectoring two-dimensional variable-area nozzles were used. For the turboshaft engines the core nozzles were axisymmetric. Eventually, detailed computational fluid dymanics (CFD) analyses would have to be performed to optimize the geometries of the inlets and the nozzles.

For the electric components, size and weight estimates were based on an electromagnetic sizing model for superconducting motors and generators[25] and on aggressive estimates for cryocoolers, inverters, and transmission lines (specific power of 14 hp/lb for the combined inverter and cryocooler, and 25 hp/lb for the transmission lines and associated electrical protection equipment).[26]

The cycle data, the material properties, and design rules for geometry, stress, turbomachinery stage-loading limits, and electrical component dimensions were used to determine an acceptable engine layout. The engine layouts for estimating performance and weights are shown in Figures 5 and 6. Propulsion system weights are summarized in Table 4.
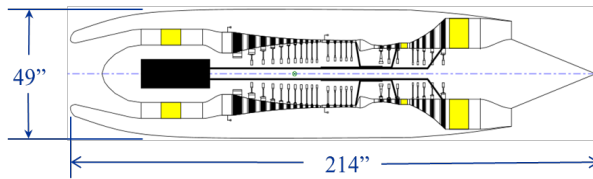

Figure 5: Turboshaft engine (3-spool) driving a superconducting generator
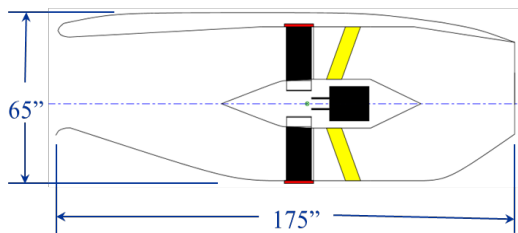

Figure 6: Superconducting-motor-driven fan installation

Table 4: Weight comparison of the N3-X/TeDP propulsion systems

	N3-X /BSCCO	N3-X /MgB$_2$
Fans - lb	7,687	7,185
Turboshafts - lb	7,529	7,103
Electrical System – lb	21,332	16,265
Inlet/Nacelles/Nozzles – lb	15,273	13,782
Total Propulsion System - lb	51,821	44,335

The electrical system of the cryocooled BSCCO system is substantially heavier than the LH$_2$ cooled MgB$_2$ system because of the weight of the cryocoolers. This is still the case when the weight of the cryogenic storage tanks to hold the LH$_2$ is included in the electrical system weight. The extra weight of the cryocoolers yields a system with a lower thrust to weight ratio than the LH$_2$ cooled system. This combined with the slightly higher fuel/energy consumption of the cryocooled system results in a heavier airplane that requires more thrust. The final result is that the turbomachinery as well as the electrical system weighs more with cryocooled system compared to the LH$_2$ cooled system.

N3-X Mission Performance

The current-generation aircraft used as a baseline for comparing the N3-X with is the Boeing 777-200LR, which has the same passenger capacity and a similar design range. A NASA model of the 777-200LR with a NASA model of the GE90-110B turbofan engine was simulated for the same payload, cruise speed, and range as the N3-X. Table 5 shows that the N3-X consumed from 70%–72% less energy depending on the type of superconducting material and cooling method than the baseline aircraft. Both exceed the NASA's N+3 goal of 60% reduction in total energy expenditure.

The key propulsion design parameters shown in Table 1 are the maximum anticipated to reach TRL 4–6 by 2025. Any change is assumed to be in the direction of lower performance. A sensitivity analysis was performed to determine how sensitive the mission energy consumption is to changes to these parameters and the results were reported by Felder, et al.[27]

The TeDP system thrust and weight have been updated from the results given in Ref. 27. The only significant change in the propulsion system configuration since the earlier study was the movement of the propulsors further aft to place the propulsor nozzle on the trailing edge. This change should only effect the sensitivities of propulsor parameters and then only by a small amount. Thus the sensitivities from the referenced study should still be applicable. Any changes in sensitivity will almost certainly not change the relative ranking of parameters with regard to total mission energy (TME) sensitivity. With the understanding that the sensitivity analysis would need to be repeated to get the most up-to-date sensitivity values, the following is a brief summary of the key findings from the referenced study.

Table 5: N3-X baseline gross takeoff weight (GTOW), mission fuel, and energy consumption compared to the Boeing 777-200LR class vehicle

Superconducting Material / Cooling Method	GTOW - lbm	Mission Fuel Consumption – lbm	Mission Energy Consumption – BTU	Mission energy reduction compared to 777-200LR
777-200LR Class Vehicle	768,000	279,800	5.20E+09	
BSCCO/Cryocooler	514,933	84,992	1.58E+09	70%
MgB_2/LH_2	496,174	76,171	1.47E+09	72%

The N3-X aircraft has a sensitivity of 1.2% increase in TME for every 1% increase in TSFC and a 0.8% increase in TME for every 10% increase in propulsion system weight. Within the propulsor module a 1% increase in total pressure loss inside the inlet results in a 3% increase in TME, and a 1% decrease in fan efficiency results in a 1% increase in TME.

Within the turboshaft engine the sensitivity of TME to changes in turbomachinery efficiency is linear over the range examined. A 1% reduction in low-pressure and high-pressure compressor efficiency results in a 0.8% and 0.4% increase in TME, respectively. A 1% reduction in efficiency of the high-pressure, low-pressure, and power turbines results in a 0.4%, 0.3%, and 0.8% increase in TME, respectively. A 50 °R reduction in compressor discharge temperature increases TME by 1%. The response of TME to changes in CMC material limit temperature is very non-linear. It is noted that the maximum gas path temperature used in the cycle design is held to 100 °R less than the maximum CMC material temperature. A 100 °R reduction from the 3460 °R baseline increases the TME by 0.2%, and the same 100 °R reduction from 2960 to 2860 °R increases TME by 1.3%. The current state of the art for uncooled CMC is about 2860 °R. Using current technology, CMCs would result in TME that is 4.8% higher than that of the baseline aircraft. So even with today's CMC materials a 68%–70% reduction in TME is possible.

The design parameter with the most uncertainty, and to which the TME is most sensitive, is the diameter of the superconducting filaments in the stator windings of the motor and generators. The baseline assumption is that both BSCCO and MgB_2 will be able to achieve a 10-µm filament diameter. The AC loss in the stator of the superconducting motors and generators is directly dependent on the diameter of the filaments. Current technology is capable of producing filaments of approximately 40 µm. A first-order analysis indicates that the energy lost in a stator

with a 40-µm filament size would be about 200% higher than that of a 10-µm filament.

Figure 7 is reproduced from the Ref. 27. It shows that a 200% increase in stator loss would result in about a 4% increase in mission energy consumption for a cryocooled BSCCO-based system. The actual losses in the stators are such a tiny fraction of the total power generated that even doubling the losses has no visible effect on TME. It is only the extra weight and power of the cryocoolers to remove these losses that affect the TME. So even with today's superconductors a 68% reduction in TME is possible.
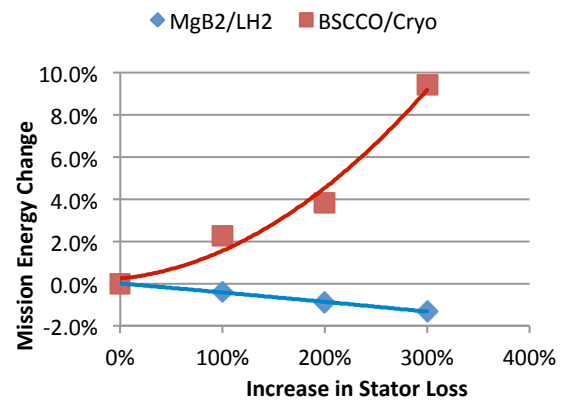

Figure 7: Mission energy change vs. percent increase in stator loss

The effect of increasing stator loss in the MgB_2/LH_2 system is not an increase in TME, but rather a counter-intuitive decrease. The apparently contradictory response is the result of the ground rule selected for the LH_2 cooling system of only carrying enough hydrogen to provide cooling. As a result, as the stator losses increased more hydrogen is required for cooling. Each pound of additional hydrogen displaces 2.7 pounds of jet fuel and so reduces the total fuel weight. The resulting reduction in total fuel weight reduces the amount of thrust required by the aircraft and so reduces the TME even though there is a very slight increase in energy lost in the electrical system. It is probable that if the ground rule limiting

the amount of hydrogen were removed, the amount of hydrogen would increase at least until all the available void space in the N3-X airframe is filled with hydrogen. It is also likely that some amount of increase in internal volume by displacing the outer mold lines would further reduce the TME consumption even though the drag of the aircraft would increase. With the very low TSEC of the TeDP system, an all-hydrogen N3-X might be possible.

Discussion

Although the TeDP vehicle N3-X features aeropropulsion-coupled devices such as a distributed BLI inlet and wing-tip mounted turboelectric generators, the current airframe used in N3-X is based on the previous N2A airframe[6] and did not start with the TeDP system from the outset. Because of the early stage of TeDP concept formulation, the aircraft development of N3-X has been delayed, and consequently the external mold-line of N3-X remains very similar to the N2A airframe except the added distributed fan nacelle and wing-tip turboelectric generators. An example of this under-developed N3-X is well illustrated in Fig. 8, where there is a CFD visualization of flow separation bubble on the top of distributed fan nacelle surface.[28] The surface contour in the figure shows the pressure distribution on the vehicle. The CFD analysis was run with an earlier configuration than what is used for the rest of the analysis, but the two configurations are similar enough that the conclusions that can be drawn from the CFD study are still valid for the later configuration.
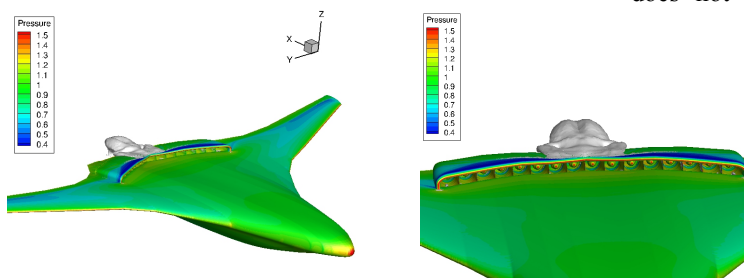

Figure 8: CFD pressure contours and visualization of flow separation bubbles near the center of nacelle at M0.84 and 35,000 ft.

As this article is being written, a separate analysis is being performed to assess the noise impact of using TeDP on the N3-X vehicle. Based on the low fan and core engine exhaust speeds in Table 3 and additional airframe noise shielding effect, it is

expected that the fan and the core jet noise levels at takeoff and landing will be significantly lower than that of the reference vehicle. However, the turboshaft machinery noise may still be high since the turboshaft engines are mounted at the wing tip and exposed to observers on the ground. If this becomes problematic in achieving the N+3 noise goal, there are several options to reduce this noise. For example, one could consider utilizing a portion of the energy in the energy storage devices used in normal operation to provide electrical load leveling and voltage regulation in order to allow the turboshaft engines to be throttled back during the vehicle takeoff phase where the low noise is most critical. The energy used for takeoff assist can be recaptured when energy is available during flight, such as during descent. Another way to reduce the turboshaft core noise is to move the core engines from the wing tip to elsewhere on the airframe to take advantage of noise shielding effect.

One key aspect of the distributed propulsion concept is that it offers a freedom of choice in propulsor types and power sources. Although the vehicle N3-X employs only one type of fan with the same diameter, the flexibility of electric power distribution enables an easy distribution of propulsors of different diameters or even the types. A concept of adding a crossflow-fan (CFF) underneath the distributed axial fans has been recently studied by Kummer[29] to ingest very low momentum boundary layer flow entering the array of propulsors. Installing the CFF reduced the flow distortion effect and increased the total pressure for the air ingested by the distributed axial fans. In terms of power source choices, N3-X currently uses only the turboelectric generators, but it does not limit the usage of other electric power sources such as battery or fuel cell as mentioned earlier.

The distributed propulsion concept usually involves a strong coupling between the aerodynamic and propulsive thrust streams, and therefore it will be necessary to design the vehicle with a multidisciplinary approach to take full advantages of PAI from the beginning of the conceptual design phase.

Concluding Remarks

To address growing aviation demands and concerns on the environment and energy usage, a revolutionary propulsion system concept called turboelectric

distributed propulsion (TeDP) is studied and presented, along with a summary of its features and issues. The TeDP system employs only a few electric generators to power multiple fans distributed on an aircraft, with strong emphasis on propulsion airframe integration (PAI) in maximizing vehicle benefits in fuel burn, noise, and other mission characteristics. In order to assess the system benefit, a notional vehicle based on a hybrid-wing-body (HWB) airframe called N3-X is configured and examined from the system-level perspective. The vehicle features two wing-tip-mounted turboelectric generators powering multiple (~14) electric fans mounted on top of a HWB airframe. The key enabling technology in the TeDP system is the lightweight, highly-efficient, electric motors, generators, and their subcomponents. In order to achieve NASA's N+3 generation aircraft goals, the vehicle N3-X uses superconducting technology in its electrical system. Because of the high electric power generation, transmission, and distribution to the multiple motor-driven fans, a study involving stability, transient response, control, and safety of a high-power electric grid was recently performed and is briefly summarized. In addition, the whole propulsion system weight, including all electric components, is estimated and used to obtain the fuel and energy usage of the vehicle for the mission specified. Depending on the cooling system required, the vehicle is expected to achieve 70%–72% reduction in energy usage relative to the current-generation reference vehicle performing the same mission. Based on the studies performed at NASA and elsewhere, it is expected that the TeDP system may indeed provide unprecedented reductions in fuel/energy consumption and community noise required in future transport aircraft.

Acknowledgements

References

1. Del Rosario, R., Follen, G., Wahls, R. Madavan, N, "Subsonic Fixed Wing Project Overview and Technical Challenges for Energy Efficient Environmentally Compatible Subsonic Transport Aircraft", 50th AIAA Aerospace Science Meeting, Nashville, TN, 9-12 Jan. 2012.

2. NASA Research and Technology Program and Project Management Requirements, NASA Procedural Requirements 7120.9. Appendix J. Technology Readiness Levels (TRLs), February 2008.

3. Kim H., Brown G. and Felder J. "Distributed Turboelectric Propulsion for Hybrid Wing Body Aircraft," 9th International Powered Lift Conference, London, United Kingdom, July 2008.

4. Liebeck, R., "Design of the Blended Wing Body Subsonic Transport", Journal of Aircraft, Vol. 41, No. 1, Jan-Feb. 2004. pp. 10-25.

5. Thomas, R., Burley, C., and Olson, E., "Hybrid Wing Body Aircraft System Noise Assessment With Propulsion Airframe Aeroacoustic Experiments," AIAA-2010-3913, 2010.

6. Kawai, R. et al. "Acoustic Prediction methodology and test validation for an efficient low-noise hybrid wing body subsonic transport," NASA Contract NNL07AA54C, Phase I Final Report PWDM08-006A, 2008.

7. Armstrong, M., Ross, C., Blackwelder, M., and Rajashekara, K., "Trade Studies for NASA N3-X Turboelectric Distributed Propulsion System Electrical Power System Architecture," SAE Int. J. Aerosp. 5(2):325-336, 2012.

8. Paschen, F., "Ueber die zum Funkenübergang in Luft, Wasserstoff und Kohlensäure bei verschiedenen Drucken erforderliche Potentialdifferenz," Annalen der Physik, vol. 273, no. 5, pp. 69 – 96, 1889.

9. Ieda, M., "Dielectric Breakdown Process of Polymers, Transactions on Electrical Insulation," IEEE, vol.EI-15, no.3, pp.206-224, June 1980.

10. Kosaki, M., "Super electrical insulation of polymers in cryogenic region," Proceedings of the 7th International Conference on Properties and Applications of Dielectric Material, vol.1, no., pp. 9- 14 vol.1, 1-5 June 2003.

11. Lee, Y., et al., "High Voltage Dielectric Characteristics of Epoxy Nano-Composites in Liquid Nitrogen for Superconducting Equipment," IEEE Transactions on Applied Superconductivity, vol.21, no.3, pp.1426-1429, June 2011.

12. Wadhwa, C. L. High Voltage Engineering. New Age International, 2007.

13. Stone, G., Boulter, E.A., Culbert., I., and Dhirani. H., Electrical insulation for rotating machines: design, evaluation, aging, testing, and repair. Vol. 21. Wiley-IEEE Press, 2004.

14. Suzuki, H., et al. "Electrical insulation property of liquid nitrogen/synthetic paper composite electrical insulation layer for high temperature superconducting cable." *Properties and Applications of Dielectric Materials, 2003. Proceedings of the 7th International Conference on*. Vol. 3. IEEE, 2003.

15. U.S. Department of Energy, "High Temperature Superconducting Cable," Presented at the S006 Annual Peer Review, Superconductivity Program for Electric Systems, Washington, DC, July 25-27, 2006. http://www.ornl.gov/sci/htsc/documents/pdf/fy2006/HTSCable-LindsayandDemko.pdf

16. Christou, I., et al., "Choice of Optimal Voltage for More Electric Aircraft Wiring Systems," IET Electrical Systems in Transportation, vol. 1, issue. 1, pp. 24-30, 2011.

17. Cotton, I., Nelms, A., and Husband, M., "Higher Voltage Aircraft Power Systems," IEEE A&E Systems Magazine, pp. 25-32, Feb. 2008.

18. Rahman, N., "Propulsion and Flight Controls Integration for the Blended Wing Body Aircraft," PhD Thesis, Cranfield University, May 2009.

19. Armstrong, M., Ross, C., Blackwelder, M., and Rajashekara, K., "Propulsion System Component Considerations for NASA N3-X Turboelectric Distributed Propulsion System," SAE Int. J. Aerosp. 5(2):344-353, 2012.

20. Claus, R., Evans, A., Lytle, J., Nichols, L., "Numerical Propulsion System Simulation," Computing Systems in Engineering, Vol. 2, No. 4, pp. 357-364, 1991.

21. NPSS User Guide Software Release: NPSS_1.6.5. http://www.npssconsortium.org

22. Tillman, T., "System Study and Distortion-Tolerant Fan Design for a boundary Layer Ingesting Propulsion System", NASA NRA NNC07CB59C Phase 2 Final Report, July 2010.

23. Tong, M. and Naylor, B., "An Object-Oriented Computer Code for Aircraft Engine Weight Estimation," GT2008-50062, ASME Turbo-Expo 2008, June 9-13, 2008.

24. Onat, E. and Klees, G., "A Method to Estimate Weight and Dimensions of Large and Small Gas Turbine Engines," NASA CR−159481, 1979.

25. Masson, P. and Ishmael, S., "NASA Glenn Superconducting Machine Sizing Model and Design Tool Development", Oct. 21, 2009, unpublished.

26. Brown, G., "Weights and Efficiencies of Electric Components of a Turboelectric Aircraft Propulsion System," AIAA-2011-225, 49th AIAA Aerospace Sciences Meeting, Orlando, FL, January 2011.

27. Felder, J., Tong, M., and Chu, J., "Sensitivity of Mission Energy Consumption to Turboelectric Distributed Propulsion Design Assumptions on the N3-X Hybrid Wing Body Aircraft", AIAA-2012-3701, 48th Joint Propulsion Conference, Atlanta, GA, USA, July 29-August 1, 2012.

28. Kim, H., and Liou, M., "Flow Simulation of N3-X Hybrid Wing Body Configuration," AIAA-2013-0221, January 2013.

29. Kummer, J., Allred, J., and Felder, J., "Hybrid Axial and Cross-Flow Fan Propulsion for Transonic Blended Wing Body Aircraft," AIAA-2012-3702, July 2012.